# Removal of catechol from water by modified dolomite: performance, spectroscopy, and mechanism

Aouda Khalfa, Senia Mellouk, Kheira Marouf-Khelifa and Amine Khelifa

## ABSTRACT

Dolomite was treated at 800 °C (D800), characterized, and used in the adsorptive removal of catechol (1,2-dihydroxybenzene) from aqueous solutions. The performances of the D800 sample, named dolomitic solid, were compared with those of the raw material. A bibliographic review shows that the data on the adsorption of phenolic compounds by dolomites are non-existent. Kinetic data, equilibrium isotherms, thermodynamic parameters, and pH influence were reported. Special attention was paid to the spectroscopic study, before and after adsorption. The purpose was to understand the mechanism of catechol uptake on dolomitic materials. Kinetics follows the pseudo-second order model. The Redlich–Peterson isotherm provides the best correlation of our isotherms. Affinity follows the sequence: D800 ≫ raw dolomite. The process is spontaneous at low temperatures and exothermic. After catechol adsorption, the shape of the band in the 3,600−3,000 $cm^{-1}$ range and its red shift towards 3,429 $cm^{-1}$ reflect a deep involvement of OH groups both of D800 and catechol, which confirm hydrogen bonding via their respective OH. On this basis, a schematic illustration was proposed. The understanding of the phenolic compound–dolomitic solid interactions constitutes a fundamental approach to developing the application of these materials in wastewater treatment.

**Key words** | adsorption, catechol, dolomite, Fourier transform infrared (FTIR) spectroscopy, mechanism, modification

**Aouda Khalfa**
**Senia Mellouk**
**Kheira Marouf-Khelifa** (corresponding author)
**Amine Khelifa**
Laboratoire de Structure, Elaboration et Applications des Matériaux Moléculaires (S.E.A.2M.), Département de Génie des Procédés,
Université de Mostaganem,
B.P. 981, R.P., Mostaganem 27000,
Algeria
E-mail: *kheira_marouf@yahoo.fr*

## INTRODUCTION

There are numerous phenolic compounds which result either from natural biosynthesis or chemical synthesis. Among the latter, catechol (1,2-dihydroxybenzene) is used as a food additive, antioxidant, cosmetic, petrochemical, pharmaceutical, etc (Suresh *et al.* 2012). This hydroxyaromatic compound is released into the environment during its use. Owing to its solubility and ubiquity in wastewaters, it disrupts aquatic life and is found to be toxic to animal, including human, cells. Catechol causes the degeneration of renal tubes, decrease of hepatic function, neurodegenerative sicknesses, and cancerous tumors (Cavalieri *et al.* 2002). Numerous methods have been employed for its removal, such as biodegradation (Subramanyam & Mishra 2007), oxidative degradation (Chien *et al.* 2009), photocatalysis (Arana *et al.* 2005). These techniques suffer from problems such as optimization of the operational parameters, partial degradation, high cost, and inadequacy for high concentration (Sharma *et al.* 2009).

Adsorption is particularly attractive due to its high effectiveness, simplicity of operation and design. Its other benefits are feasibility for both batch and continuous processes and formation of little sludge (Suresh *et al.* 2011). Many materials have been used to remove catechol from synthetic solutions, such as hematite (Saikia *et al.* 2013), activated carbon (Suresh *et al.* 2011) and aluminium hydroxide (Guan *et al.* 2006). These adsorbents were found to be expensive along with disadvantages caused by their later treatment and regeneration.

Dolomite is an important industrial mineral. Its structure contains alternating planes of $Mg^{2+}$ and $Ca^{2+}$ cations, with a theoretical formula of $CaCO_3.MgCO_3$. A bibliographic review shows that there is no study dealing with the elimination of phenolic compounds by dolomites and their modified forms. This study was undertaken to evaluate the potential of modified dolomite for removing catechol from synthetic solutions. Accordingly, Algerian

doi: 10.2166/wst.2018.071

dolomite was heated at 800 °C and characterized by thermal analysis, scanning electron microscopy (SEM), and nitrogen adsorption. The removal of catechol was studied by considering contact time, solution concentration, temperature, and pH. Particular interest was focused on the spectroscopic study. Fourier transform infrared (FTIR) spectroscopy was used to examine the interaction between the catechol molecule and the dolomitic surface. The objective was to elucidate the mechanism of the adsorption of this hydroxyaromatic compound. The understanding of the phenolic compound–dolomitic solid interactions is fundamental to developing the application of these materials in wastewater treatment.

## MATERIALS AND METHODS

### Materials

The dolomite used in this paper was mined from a deposit found in eastern region of Algeria, and particle sizes of 0.125–0.25 mm were used. The material was calcined at 800 °C for 2 hours. This duration suffices to induce transformations in the bulk of many materials (Bessaha *et al.* 2016). In this paper, the abbreviation D800 is used (D for dolomite; 800 process temperature in °C). D800 are called dolomitic solid in this study because its properties are different from those of raw dolomite.

### Characterization

A chemical analysis of the untreated sample gave: 31.18% CaO, 21.05% MgO, 0.02% $Fe_2O_3$, 0.01% $SiO_2$, 0.002% $Al_2O_3$, 0.0015% $MnO_2$, and 0.01% $Cr_2O_3$. Differential and gravimetric thermal analyses (DTA and TG) were simultaneously carried out on an SDT Q600 TA instrument. Approximately 40 mg of the raw dolomite was heated in an alumina crucible at a rate of 10 °C $min^{-1}$, under a dry air flow of 50 mL $min^{-1}$. The surface modifications of the raw dolomite and D800 were observed using a Jeol, JSM-6360 scanning electron microscope. The assessment of specific surface area was carried out by $N_2$ adsorption at 77 K via an ASAP 2010 Micromeritics. The samples were first out-gassed under secondary vacuum at 623 K for 12 hours. Pore size distribution was calculated from the desorption branch using the Barrett–Joyner–Halenda method. A Shimadzu Prestige spectrophotometer was used to collect IR spectra at a resolution of 4 $cm^{-1}$ between 4,000 and 400 $cm^{-1}$. KBr pellets containing 0.5 wt% of solid sample were used for transmission studies.

### Adsorption procedure

A series of catechol (CAS N°: 120-80-9, linear chemical formula: $C_6H_4$–1,2-$(OH)_2$, FW: 110.11 g $mol^{-1}$, $\lambda_{max}$: 275 nm, supplied by Sigma-Aldrich) solutions of known concentration were prepared from a stock solution of 1 g $L^{-1}$. Batch experiments were carried out by mixing 80 mg of the dolomitic solid with 20 mL of aqueous catechol solution. This solid/solution ratio was used after optimization. After each experiment, the solution was separated by filtration. The estimation of the amount adsorbed was performed via a Shimadzu 1240 UV–vis spectrophotometer, at 275 nm, by subtracting the concentration of the supernatant after adsorption from the initial concentration. The influence of pH, contact time, temperature, and concentration was evaluated. The experimental parameters are outlined in Table 1.

### Theoretical approach

#### Kinetics

Different equations were used to model the kinetic data. Among these, Lagergren (1898) proposed a pseudo-first order kinetic model. The integral form of the model is:

$$\log(Q_e - Q_t) = \log Q_e - \frac{K_1 t}{2.303} \quad (1)$$

where $Q_t$ (mg $g^{-1}$) is the amount adsorbed at time $t$, $Q_e$ (mg $g^{-1}$) the adsorption capacity at equilibrium, $K_1$ ($min^{-1}$) the

**Table 1** | Experimental conditions during the adsorption of catechol

| | |
|---|---|
| Contact time | 1, 3, 5, 10, 20, 40, 60, 120, 240 min; $C_{initial}$ = 200 mg $L^{-1}$ [solid]/[solution]: 4 g $L^{-1}$; T: 25; pH: 7 |
| Concentration | 20, 60, 100, 150, 200, 400, 600 mg $L^{-1}$ [solid]/[solution]: 4 g $L^{-1}$; contact time: 2 h; pH: 7 |
| Temperature | 25, 40 and 55 °C, [solid]/[solution]: 4 g $L^{-1}$; contact time: 2 h; pH: 7 |
| pH | pH 3.0 – 5.0 – 7.0 –9.0 – 11.0 [solid]/[solution]: 4 g $L^{-1}$; contact time: 2 h; T: 25 °C |

pseudo-first order rate constant, and $t$ (min) is the contact time.

Kinetics may also be described by a pseudo-second order reaction. The linearized form of the model is (Ho & McKay 1999):

$$\frac{t}{Q_t} = \frac{1}{K_2 Q_e^2} + \frac{t}{Q_e} \tag{2}$$

where $K_2$ (g mg$^{-1}$ min$^{-1}$) is the pseudo-second order rate constant. The initial adsorption rate ($h$) as $t \to 0$ can be defined as:

$$h = K_2 . Q_e^2 \tag{3}$$

The plot of $t/Q_t$ vs. $t$ should yield a straight line, from which $K_2$ and $h$ can be calculated from the slope and intercept.

When adsorption in batch mode is used, the intraparticle diffusion is often the rate-controlling step. Its equation is given by (Weber & Morris 1963):

$$Q_t = K_{id} t^{1/2} + C \tag{4}$$

where $K_{id}$ (mg g$^{-1}$ min$^{-1/2}$) is the intraparticle diffusion rate and $C$ is a constant. The values $K_{id}$ and $C$ are determined from the slope and intercept, respectively.

### Isotherms modeling

Equilibrium data were correlated to the Langmuir, Freundlich, and Redlich–Peterson (RP) models. The Langmuir equation can be represented by (Langmuir 1918):

$$\frac{C_e}{Q_e} = \frac{1}{Q_m . K_L} + \frac{C_e}{Q_m} \tag{5}$$

where $Q_e$ (mg g$^{-1}$) is the equilibrium amount adsorbed, $C_e$ (mg L$^{-1}$) the equilibrium concentration, $K_L$ (L mg$^{-1}$) a constant related to the affinity of binding sites, and $Q_m$ (mg g$^{-1}$) the amount adsorbed for a complete monolayer coverage.

The Freundlich model has been widely used and may be written as (Freundlich 1906):

$$\log Q_e = \log K_F + \frac{1}{n} \log C_e \tag{6}$$

where $K_F$ (L g$^{-1}$) is a constant taken as an indicator of adsorption capacity and $1/n$ a constant indicative of the intensity of adsorption.

The three-parameter Redlich–Peterson (RP) (1959) model has been used to improve the fit by the equations of Langmuir or Freundlich. Its equation is as follows:

$$Q_e = \frac{K_{RP} C_e}{1 + a_{RP} C_e^{\beta}} \tag{7}$$

where $Q_e$ (mg g$^{-1}$) is the amount adsorbed at equilibrium, $C_e$ (mg L$^{-1}$) the concentration at equilibrium, $K_{RP}$ (L g$^{-1}$) and $a_{RP}$ (mg L$^{-1}$)$^{-\beta}$ the constants of the Redlich–Peterson model, and $\beta$ the heterogeneity factor that depends on the surface properties of the material.

### Thermodynamics

The thermodynamic parameters $\Delta H^0$, $\Delta S^0$, and $\Delta G^0$ were calculated using the following equation:

$$\ln K_d = \left(-\Delta H^0 / R.T\right) + \left(\Delta S^0 / R\right) \tag{8}$$

where $\Delta H^0$ and $\Delta S^0$ are the changes in enthalpy (kJ mole$^{-1}$) and entropy (kJ mole$^{-1}$ K$^{-1}$), respectively, T the absolute temperature (K), R gas constant (J mol$^{-1}$ K$^{-1}$), and $K_d$ (L g$^{-1}$) the distribution coefficient. This coefficient reflects the overall catechol–material affinity and is given by:

$$K_d = Q_e / C_e \tag{9}$$

The enthalpy and entropy changes are calculated by plotting ln $K_d$ versus 1/T, which gives a straight line. According to thermodynamics, the Gibbs free energy change, $\Delta G^0$, is related to $\Delta H^0$ and $\Delta S^0$ at constant temperature by the following equation:

$$\Delta G^0 = \Delta H^0 - T\Delta S^0 \tag{10}$$

## RESULTS AND DISCUSSION

### Characterization

The DTA and TG curves of the raw dolomite are shown in Figure 1. In the range 25–1,000 °C, the DTA curve shows one endotherm centered at 755 °C. The shape of the DTA curve from 500 °C reveals that our dolomite decomposes

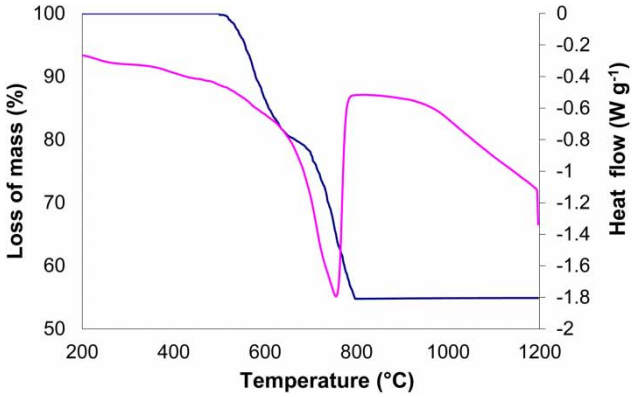


**Figure 1** | DTA and TG curves of the raw dolomite.

under air in one stage, as follows:

$$CaMg(CO_3)_2 \rightarrow CaO + MgO + 2CO_2 \quad (11)$$

Otsuka (1986) showed that dolomite undergoes decomposition in two steps if the partial pressure of $CO_2$ is above 100 mm Hg. As we used a sample of 40 mg, the partial pressure of $CO_2$ during decomposition can only be low. Rodriguez-Navarro *et al.* (2012) demonstrated that the concept of 'half decomposition' that consists in the formation of MgO and $CaCO_3$ has no mechanistic significance, but there is a direct decomposition in MgO and CaO oxides in one stage. The endotherm centered at 755 °C starts from *ca.* 500 °C and joins the baseline at *ca.* 790 °C. This means that from 800 °C the sample undergoes no decomposition.

The TG curve shows a continuous loss of mass between 500 and 800 °C with a concavity change at *ca.* 700 °C. This singular point at 700 °C would concern the removal of $CO_2$ combined with $MgCO_3$. A total loss of 45.2% was found between 500 to 800 °C, in close agreement with the 46.2% reported by Shahraki *et al.* (2009). From TG and derivative thermogravimetry (DTG) curves, Wang *et al.* (2015) also showed that the calcination of dolomite occurs in one stage and is complete at 800 °C, generating mixed CaO–MgO oxides.

SEM images of dolomite and D800 are shown in Figure 2. The SEM analysis of dolomite indicates the presence of cleavages and shows an apparent preferential orientation of dolomite crystals along the c-axis. Dolomite belongs to the rhombohedral crystalline system, which has a threefold inversion axis and is therefore anisotropic (De Aza *et al.* 2002). After thermal modification, significant changes in the surface topography of D800 happen. The corresponding micrograph highlights the newly created pores and slots. The structure appears to be less compact than that of the raw material.

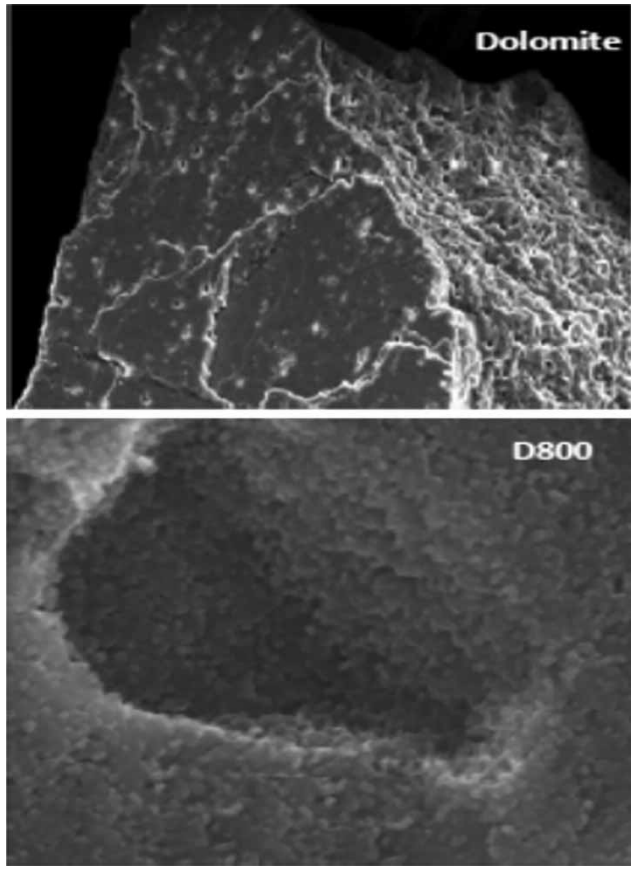


**Figure 2** | SEM images of dolomite and D800.

These features could be explained by the decarbonation of $MgCO_3$ and $CaCO_3$ in raw dolomite. The release of $CO_2$ leads to a more porous structure.

## Dolomite

Results relating to the specific surface area of the raw dolomite and D800 gave 0.79 and 31.89 $m^2 g^{-1}$, respectively. This demonstrates that the best temperature for full calcination is 800 °C. The surface area of D800 is 40 times higher than that of raw dolomite. The pore size distribution diagram of D800 is shown in Figure 3. We could not determine that of untreated dolomite because its specific area is insignificant. The distribution of D800 pores is multimodal. Each mode corresponds to a maximum of the curve. The diagram shows three distinct modes centered on pores radii of 4.98, 10.30, and 14.17 nm, which confirms a mainly mesoporous character. The intensity of these maxima is unequally distributed, indicating that the treatment of dolomite at 800 °C led to a heterogeneous microtexture.

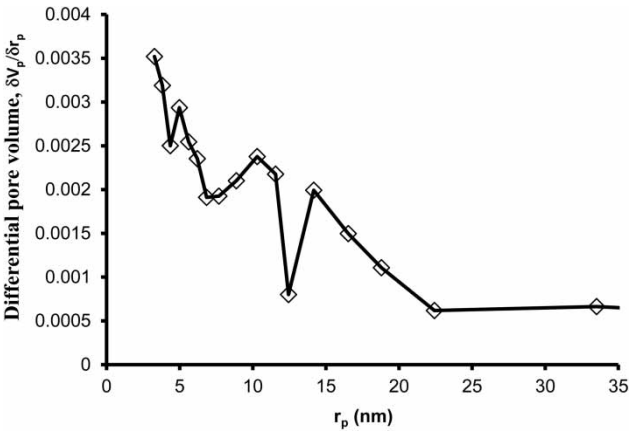


**Figure 3** | Diagram of pore size distribution of D800.

## Catechol adsorption

### Kinetics

The effect of contact time on the adsorption of catechol by raw dolomite and D800 is shown in Figure 4. The rate of adsorption is fast in the first 10 min, then it diminishes continuously, reaching an equilibrium at about 2 hours. So, this duration is sufficient to study equilibrium data. Rapid initial adsorption could be attributed to the presence of numerous available adsorption sites and a high gradient of solute concentrations. Saikia *et al.* (2013) also showed that catechol uptake by hematite reaches a plateau after 120 min.

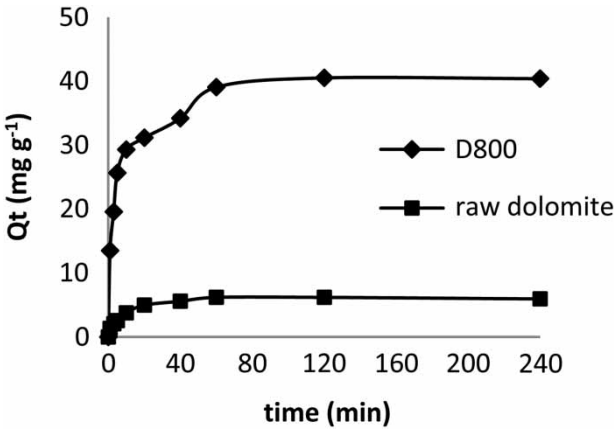


**Figure 4** | Kinetics of catechol adsorption on D800 and raw dolomite.

Pseudo-first order, pseudo-second order, and intraparticle diffusion models were examined to understand the mechanism of adsorption. The parameters relating to these models are summarized in Table 2. The pseudo-first order equation was considered inappropriate because the values of the determination coefficient, $R^2$, are low and the experimental (Qe(exp)) and theoretical (Qe(cal)) quantities diverge considerably. The experimental kinetic data were correlated using the pseudo-second order equation. Indeed, the plots of t/Qt against t (Equation (2)) gave straight lines (data not shown), corresponding to $R^2$ values >0.99. The $Q_e$(cal) and $Q_e$(exp) values are closely related. Considering the initial rate, *h*, D800 adsorbs faster than raw dolomite. This rate is seven times higher and is caused by the dolomite decarbonation, which facilitates the diffusion of catechol molecules. When adsorption in batch mode is used, the possibility of intraparticle diffusion is often present. Its application necessitates the plotting of Qt against $t^{1/2}$, which should give a linear relationship. If the straight line passes through the origin, intraparticle diffusion will be the sole rate-limiting process. As *C* values are different from zero (Table 2), intraparticle diffusion is not the only step which controls rate. The *C* value provides an insight into the thickness of the boundary layer, i.e., the larger the intercept, the greater the boundary layer effect. The *C* value of D800 is 13 times larger than that of raw dolomite. Thermal treatment disrupts the interfacial properties of dolomitic solids, so that the effect of the boundary layer plays a major role in catechol adsorption.

### Isotherms at equilibrium

The isotherms of catechol adsorption at 25, 40, and 55 °C are shown in Figure 5. The extent of adsorption decreases with increasing temperature. For example, D800 adsorbs 68.2 and 20.8 mg $g^{-1}$ at 25 and 55 °C, respectively, which

**Table 2** | Kinetic parameters for catechol adsorption on raw dolomite and D800.

| | | | Pseudo-first order model | | | Pseudo-second order model | | | | Intraparticle diffusion model | | |
|---|---|---|---|---|---|---|---|---|---|---|---|---|
| Samples | T (°C) | $Q_e$(exp) (mg $g^{-1}$) | $Q_e$(cal) (mg $g^{-1}$) | $K_1$ ($min^{-1}$) | $R^2$ | $Q_e$(cal) (mg $g^{-1}$) | $K_2$ (g $mg^{-1}$ $min^{-1}$) | *h* (mg $g^{1}$ $min^{-1}$) | $R^2$ | $K_{id}$ (mg $g^{-1}$ $min^{-1/2}$) | *C* (mg $g^{-1}$) | $R^2$ |
| Raw dolomite | 25 | 6.21 | 2.63 | 0.011 | 0.698 | 6.16 | 0.04 | 1.46 | 0.999 | 0.624 | 1.64 | 0.925 |
| D800 | 25 | 40.51 | 15.32 | 0.022 | 0.930 | 40.15 | 0.006 | 10.11 | 0.999 | 2.21 | 21.29 | 0.970 |

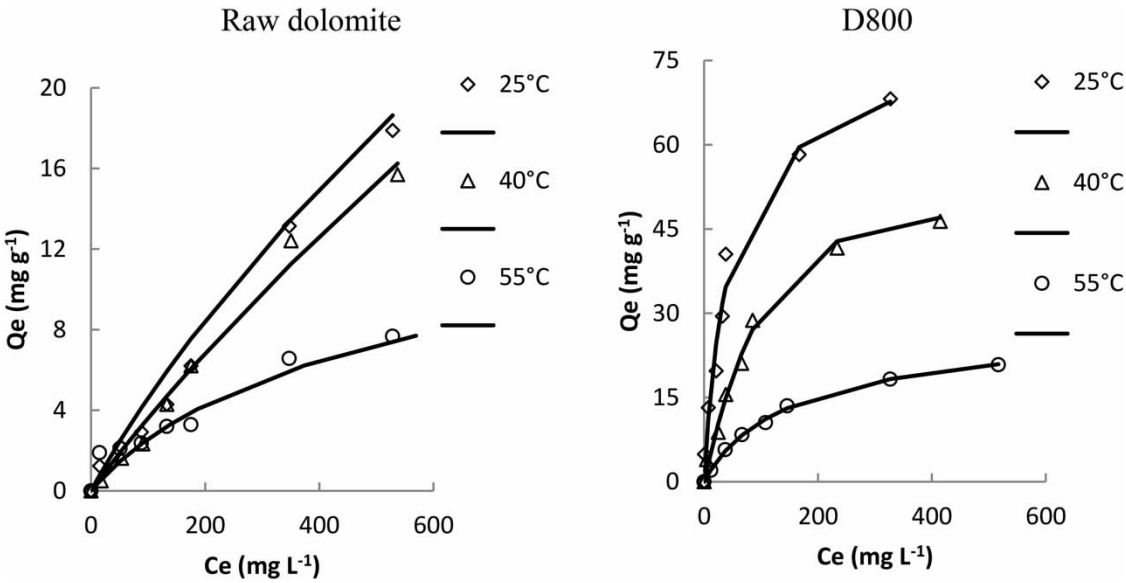


**Figure 5** | Isotherms according to the RP model (—) and experimental data (diamonds, triangles, circles) for raw dolomite and D800.

implies a physical process. Affinity follows the sequence: D800 ≫ raw dolomite, regardless of temperature. The decomposition of dolomite into MgO and CaO and a specific area 40 times larger would explain why D800 adsorbs much more than raw dolomite.

Using the classification of Giles *et al.* (1960), the isotherms of dolomite are S-shaped. The initial part of this curve type reveals few interactions between catechol and the solid. As the concentration increases, adsorption occurs more easily: the molecules adsorbed at low concentrations facilitate the adsorption of additional molecules via attractive adsorbate–adsorbate interactions. Calcination at 800 °C transforms the isotherms from S- to L-shaped, indicating a high affinity of D800 towards catechol from the lowest concentrations.

The fitting of experimental isotherms to appropriate models represents a good data analysis tool. Langmuir, Freundlich, and Redlich−Peterson models were used and their parameters gathered in Table 3. To test the validity of a model, we were interested in the determination coefficient ($R^2$) and the average relative error (E%). The Langmuir model was found to be unsuitable because a $R^2$ value as low as 0.068 was obtained for raw dolomite, while the error values are globally >10% for D800. The inadequacy of this model can be explained from its assumptions: it is improbable that all adsorption sites on dolomitic solids are both identical and energetically equivalent. The correlation of data with the Freundlich isotherm is slightly better. Even if the values of determination coefficient are broadly higher than 0.95, those of errors are almost all higher than 10%. This would confirm the previous observations that the Freundlich model correlates fairly well with the isotherms at low concentrations and diverges at higher concentrations.

The Redlich–Peterson (1959) model uses three adjustable parameters and can be applied to both homogeneous and

**Table 3** | Adjustable parameters of the models used for catechol adsorption on raw dolomite and D800

| | | Langmuir model | | | | Freundlich model | | | | Redlich–Peterson model | | | | |
|---|---|---|---|---|---|---|---|---|---|---|---|---|---|---|
| **Samples** | **T (°C)** | **$Q_m$ (mg g$^{-1}$)** | **$K_L$ (L mg$^{-1}$)** | **$R^2$** | **E (%)** | **$K_F$ (L g$^{-1}$)** | **n** | **$R^2$** | **E (%)** | **$K_{RP}$ (L g$^{-1}$)** | **$\beta$** | **$a_{RP}$ (mg L$^{-1}$)$^{-\beta}$** | **$R^2$** | **E (%)** |
| Raw dolomite | 25 | 58.82 | 0.0009 | 0.282 | 17.6 | 0.37 | 1.22 | 0.952 | 17.1 | 0.0548 | 0.6435 | 0.0098 | 0.965 | 18.2 |
| | 40 | −166.7 | −0.00017 | 0.068 | 10.3 | 0.024 | 0.95 | 0.990 | 8.9 | 0.0400 | 0.6508 | 0.0054 | 0.986 | 13.6 |
| | 55 | 10.10 | 0.0044 | 0.778 | 24.6 | 0.53 | 2.60 | 0.821 | 20.6 | 0.0338 | 0.8959 | 0.0051 | 0.951 | 9.2 |
| D800 | 25 | 74.08 | 0.028 | 0.981 | 22.4 | 6.61 | 2.40 | 0.970 | 11.6 | 1.8374 | 0.9537 | 0.0315 | 0.977 | 9.8 |
| | 40 | 57.8 | 0.010 | 0.973 | 13.3 | 1.74 | 1.74 | 0.964 | 13.0 | 0.4518 | 1.2393 | 0.0017 | 0.992 | 6.1 |
| | 55 | 26.6 | 0.007 | 0.998 | 2.5 | 0.56 | 1.64 | 0.960 | 13.8 | 0.1952 | 0.9321 | 0.0113 | 0.998 | 2.6 |

heterogeneous systems. In view of the $R^2$ and E% values (Table 3), the Redlich–Peterson isotherm efficiently describes catechol adsorption on dolomitic adsorbents, except for some average errors for raw dolomite. The RP equation also correlated to the adsorption of catechol on activated carbons (Suresh *et al.* 2011). The $\beta$ parameter is overall lower than 1, reflecting a favorable adsorption of this phenolic derivative on highly heterogeneous sites. Stefaniak *et al.* (2002) showed that different causes are responsible for the heterogeneity of the dolomitic surfaces, among which are crystallographic defects, the chemistry of adsorption sites, and the influence of neighboring sites. The Redlich–Peterson constant, $K_{RP}$, gives an indication of the adsorption capacity. The $K_{RP}$ values decrease with increasing temperature and are markedly higher for D800, in line with the evolution of the isotherms. To illustrate the values of Table 3, the experimental and theoretical data were compared in Figure 5. The Redlich–Peterson equation provides a good description of the experimental isotherms. However, some points for the raw dolomite diverge from the theoretical points, which impacts on the average relative error. This divergence would be explained by the shape of the isotherm obtained. The isotherms of dolomite are S-shaped, indicating the prevalence of the adsorbate–adsorbate attraction, unlike $\beta$ values that reveal heterogeneous adsorbate–adsorbent interactions.

## Comparison with other adsorbents

The values of the maximum adsorption capacity of different adsorbents to catechol are listed in Table 4. The results show that D800 has a great capacity–higher than for adsorbents such as alumina, waste Fe(III)/Cr(III) hydroxide, activated carbon, and bentonite. Therefore D800 appears to be very effective for removing catechol from wastewaters.

**Table 4** | Comparison of uptake capacities of catechol for different adsorbents

| Adsorbent | Qm (mg $g^{-1}$) | Reference |
|---|---|---|
| $\alpha$-alumina | 2.4 | Borah *et al.* (2011) |
| Waste Fe(III)/Cr(III) hydroxide | 4.0 | Namasivayam & Sumithra (2004) |
| Multiwalled carbon nanotubes | 14.2 | Liao *et al.* (2008) |
| Organophilic bentonite | 49.8 | Shakir *et al.* (2008) |
| D800 | 74.1 | Present study |

## Thermodynamic parameters

The thermodynamic data resulting from Equations (8–10) are listed in Table 5. The negative $\Delta H^0$ values show that the adsorption of catechol is exothermic. Released heat is much larger for D800. The negative values of $\Delta S^\circ$ indicate much more ordered adsorbate–adsorbent systems, for which the number of degrees of freedom at the phenolic compound–dolomitic material interface decreases after adsorption. The greater the release of heat, the greater the entropy value. The adsorption of catechol on dolomite occurs spontaneously. For D800, the process is spontaneous at 25 °C and tends towards non-spontaneity with increasing temperature. However, the positive values of $\Delta G^0$ at 40 and 55 °C, combined with the negative values of $\Delta H^0$ and $\Delta S^0$, indicate that adsorption would be spontaneous at low temperatures. Knowing that the change in free energy for chemisorption is in the range 80–400 kJ $mol^{-1}$. the values of $\Delta G$ obtained in this study suggest that catechol is physisorbed on dolomitic solids.

## Effect of pH

The influence of pH was studied for raw dolomite and D800 (Figure 6). pH increases rapidly from 3 to 7, beyond which it

**Table 5** | Thermodynamic data for catechol adsorption on raw dolomite and D800

| Adsorbents | $\Delta H^\circ$ (kJ $mole^{-1}$) | $\Delta S^\circ$ (kJ $mole^{-1}$ $K^{-1}$) | $\Delta G^\circ$ (kJ $mole^{-1}$) | | |
|---|---|---|---|---|---|
| | | | 25 °C | 40 °C | 55 °C |
| Raw dolomite | −6.2 | −0.049 | −8.4 | −9.1 | −9.8 |
| D800 | −54.3 | −0.182 | −0.2 | 2.7 | 5.4 |

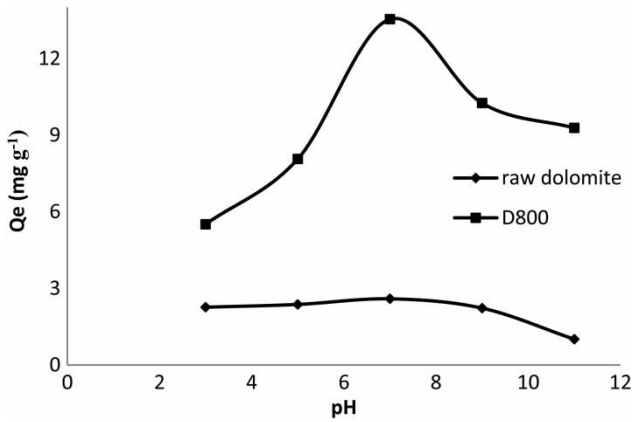


**Figure 6** | Effect of pH on the adsorption of catechol on raw dolomite and D800.

decreases. Thus, the capacity of D800 at pH 3, 7, and 11 is 5.5, 13.5, and 9.3 mg $g^{-1}$, respectively. This adsorption cannot be explained by electrostatic attraction because catechol exists exclusively in molecular form up to pH 7. Also, the isoelectric point of dolomite is 6.2, i.e. close to the pH of this study. Moreno-Piraján *et al.* (2012) found that the best adsorption of catechol on activated carbons occurs at pH 7, Suresh *et al.* (2011) suggested that the interaction of catechol with granular activated carbon, at neutral pH, occurs through hydrogen bonding. Gulley-Stahl *et al.* (2010) showed that catechol forms an outer-sphere complex on $MnO_2$ and an inner-sphere complex on $Fe_2O_3$, $TiO_2$, and $Cr_2O_3$.

## FTIR analysis

FTIR spectroscopy analysis was used to understand the adsorption mechanism. The IR spectra of D800 and catechol, before and after adsorption (catechol/D800), were collected in the 4,000–400 $cm^{-1}$ interval (Figure 7). The spectrum of D800 (Figure 7–D800) shows a sharp and intense band at 3,633 $cm^{-1}$ attributed to the stretching vibration of the hydroxyl groups associated with Ca in $Ca(OH)_2$ (Gunasekaran & Anbalagan 2007). Fujimori *et al.* (2016) reported that the hydration of CaO into $Ca(OH)_2$ occurs from exposure to water at $1 \times 10^{-4}$ Torr. When charred dolomite is again exposed to air, i.e., to negligible amounts of $H_2O$ and $CO_2$ vapors, numerous spectral features which were removed by thermal treatment are recovered (Ji *et al.* 2009). Accordingly, the bands at 1,439, 873, and 712 $cm^{-1}$ are caused by recovered $CO_2$, i.e, by the appearance of the $v_3$ (asymmetric stretching), $v_2$ (out-of-plane bending), and $v_4$ (in-plane bending) modes of $CO_3^{2-}$, respectively (Pokrovsky *et al.* 2000). The 1,381 $cm^{-1}$ band is also due to recovered $CO_2$. In this sense, the bands at 1,571 and 1,627 $cm^{-1}$ are assigned to OH bending (Madejova *et al.* 2010).

The catechol spectrum (Figure 5–catechol) highlights a band at 3,446 $cm^{-1}$ corresponding to bonded OH stretching. The aromatic character of our compound appears at 1,622, 1,512, and 1,469 $cm^{-1}$. It corresponds to aromatic C = C stretches, i.e., to C = C in-plane vibrations. The band at 1,366 $cm^{-1}$ is due to OH in-plane bending. Those at 1,251

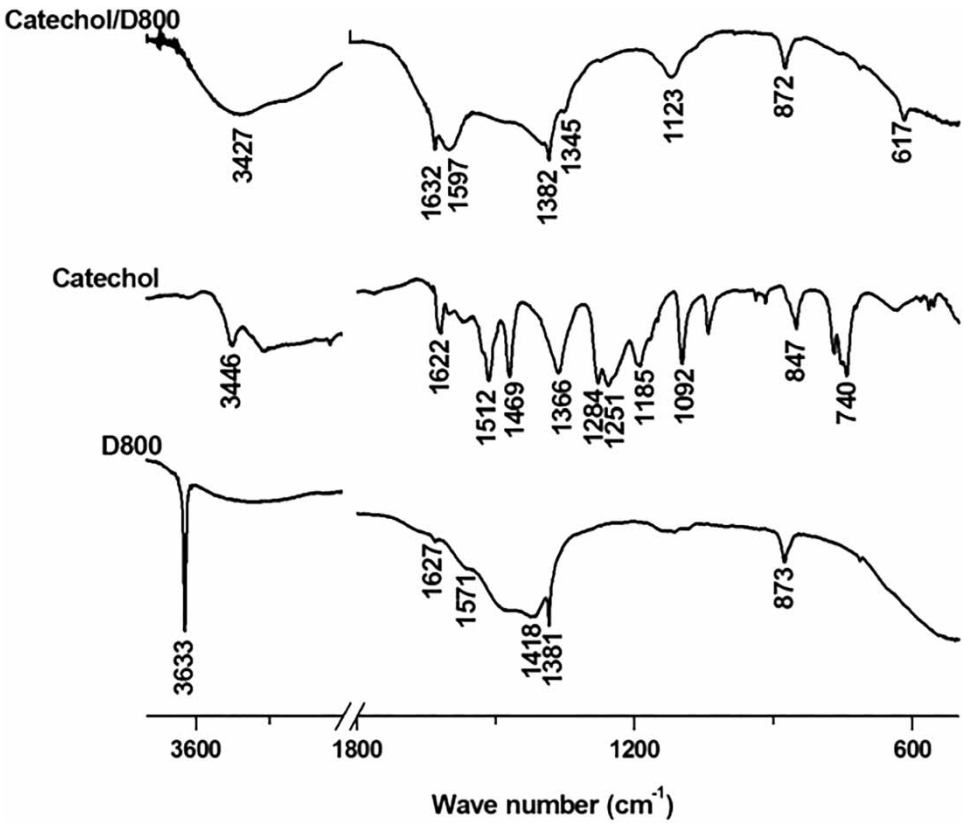


**Figure 7** | FTIR of D800, catechol, and catechol-loaded D800.

and 1,185 $cm^{-1}$ are the consequence of C – OH stretching. The strong band appearing at 1,284 $cm^{-1}$ may be linked to the coupling of C – O stretching with O – H in-plane deformation. The peaks at 1,092 and 847 $cm^{-1}$ characterize the in-plane and out-of-plane deformations of C – H, while that at 740 $cm^{-1}$ is assigned to the out-of-plane bending of O – H. The assignment of the catechol bands was carried out from different references (Mistry 2009).

After exposure to a solution of 100 mg $L^{-1}$ of catechol at pH 7, the spectrum of catechol-loaded D800 (Figure 5–catechol/D800) displays some modifications: a certain number of bands disappear whilst others shift. These spectral characteristics highlight the interaction of the catechol molecule with the D800 surface. A broad band in the 3,600–3,000 $cm^{-1}$ range with a maximum at 3,427 $cm^{-1}$ appears, indicating the formation of OH stretching. The shape of the band and its red shift denote a deep involvement of OH groups both of D800 and catechol. Thus, catechol and D800 confirm hydrogen bonding via their respective OH. On the basis of the discussion above (Figure 5–D800), it is about OH combined with Ca in $Ca(OH)_2$ (D800). When hydrogen bonding occurs, both stretching and bending vibrations move to lower frequencies with band widening: the band associated with OH in-plane bending (1,366 $cm^{-1}$, Figure 7–catechol) shifts to 1,345 $cm^{-1}$.

## Mechanism

Catechol is capable of interacting with the surface of dolomitic solids via different mechanisms such as inner-sphere complexation, outer-sphere complexation and/or hydrogen bonding. We can discount inner-sphere complexation because all the measured parameters show that catechol is physisorbed. Also, no peak was found to increase its intensity in the 1,512–1,469 $cm^{-1}$ and 1,251–1,185 $cm^{-1}$ ranges, refuting once again the formation of inner-sphere complexation on the D800 surface. In addition, there are significant differences at pH 7 between the spectra of catechol adsorbed on D800 and catechol in solution, suggesting that the contribution of outer-sphere complexation is negligible (Johnson *et al.* 2004). In this context, the outer-sphere mode was found to be prevalent at high pH for an adsorption largely governed by electrostatic interactions. The fact that our experiments were carried out at pH 7 would suggest that the mechanism of catechol uptake takes place via hydrogen bonding, as a consequence of the spectroscopic study. When catechol is adsorbed through hydrogen bonding, it interacts directly on D800 surface sites, whilst once it adsorbs via an outer-sphere complexation, it interacts with the solvation shell of surface sites (Bargar *et al.* 1999). Lana-Villarreal *et al.* (2005) reported that the adsorption of catechol on metal oxide via hydrogen bonding intervenes between the hydrogen of the adsorbate and the oxygen of the adsorbent.

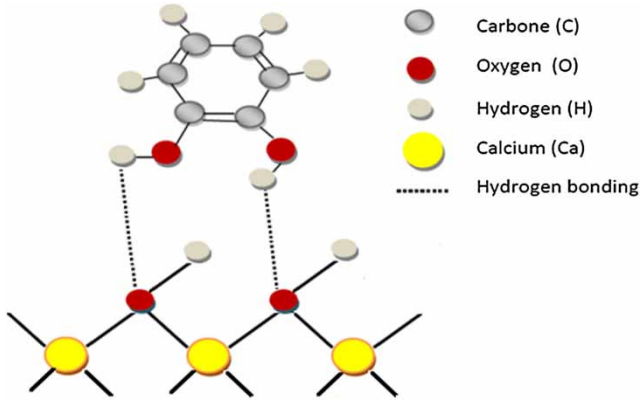


**Figure 8** | Mechanism of interaction between catechol and surface sites of dolomite heated to 800 °C.

From FTIR spectroscopy (Figure 7–catechol/D800), we found that catechol interacts with $Ca(OH)_2$ sites via hydrogen bonding. Knowing that the band whose the maximum appears at 3,429 $cm^{-1}$ is strong and broad relates it to polymeric intermolecular hydrogen bonding (Mistry 2009). In other words, catechol would interact via its two hydroxyl groups with the two hydroxyls associated with Ca in D800. Such a mechanism is depicted in Figure 8.

## CONCLUSION

The thermal treatment of dolomite at 800 °C (D800) leads to its full calcination and a specific surface 40 times larger than that of raw dolomite. The kinetics of catechol adsorption follows the pseudo-second order kinetics with some intraparticle diffusion. The isotherms are S-shaped for dolomite and change to L-shaped after calcination. They are efficiently described with the Redlich–Peterson model. Affinity follows the sequence: D800 ≫ raw dolomite. The process is spontaneous at low temperatures and exothermic. The spectroscopic study highlights a physical interaction via hydrogen bonding. The two neighboring hydroxyl groups of catechol interact with the two hydroxyls associated with Ca ($Ca(OH)_2$ sites) in D800.

## REFERENCES


Arana, J., Rodriguez, C. F., Diaz, O. G., Melian, J. A. H. & Pena, J. P. 2005 Role of Cu in the Cu–$TiO_2$ photocatalytic degradation of dihydroxybenzenes. *Catal. Today* **101**, 261–266.

Bargar, J. R., Persson, P. & Brown Jr, G. E.. 1999 Outer-sphere adsorption of Pb(II) EDTA on goethite. *Geochim. Cosmochim. Acta* **63**, 2957–2969.

Bessaha, F., Marouf-Khelifa, K., Batonneau-Gener, I. & Khelifa, A. 2016 Characterization and application of heat-treated and acid-leached halloysites in the removal of malachite green: adsorption, desorption, and regeneration studies. *Desalin. Water Treat.* **57**, 14609–14621.

Borah, J. M., Sarma, J. & Mahiuddin, S. 2011 Adsorption comparison at the $\alpha$-alumina/water interface: 3,4-dihydroxybenzoic acid vs. catechol. *Colloids and Surfaces A: Physicochem. Eng. Aspects* **387**, 50–56.

Cavalieri, E. L., Li, K. M., Balu, N., Saeed, M., Devanesan, P., Higginbotham, S., Zhao, J., Gross, M. L. & Rogan, E. G. 2002 Catechol ortho-quinones: the electrophilic compounds that form depurinating DNA adducts and could initiate cancer and other diseases. *Carcinogenesis* **23**, 1071–1077.

Chien, S. W. C., Chen, H. L., Wang, M. C. & Seshaiah, K. 2009 Oxidative degradation and associated mineralization of R, hydroquinone and resorcinol catalyzed by birnessite. *Chemosphere* **74**, 1125–1133.

De Aza, A. H., Rodriguez, M. A., Rodriguez, J. L., De Aza, S., Pena, P., Convert, P., Hansen, T. & Turrillas, X. 2002 Decomposition of dolomite monitored by neutron thermodiffractometry. *J. Am. Ceram. Soc.* **85**, 881–888.

Freundlich, H. M. F. 1906 Over the adsorption in solution. *J. Phys. Chem.* **57**, 385–470.

Fujimori, Y., Zhao, X., Shao, X., Levchenko, S. V., Nilius, N., Sterrer, M. & Freund, H. J. 2016 Interaction of water with the CaO(001) surface. *J. Phys. Chem. C* **120**, 5565–5576.

Giles, C. H., Mac Ewan, T. H., Makhwa, S. N. & Smith, D. J. 1960 Studies in Adsorption. Part XI.* A System of Classification of Solution Adsorption Isotherms, and its Use in Diagnosis of Adsorption Mechanisms and in Measurement of Specific Surface Areas of Solids. *J. Chem. Soc.* **93**, 3973.

Guan, X. H., Li, D. L., Shang, C. & Chen, G. H. 2006 Role of carboxylic and phenolic groups in NOM adsorption on minerals: a review. *Water Science & Technology: Water Supply* **6**, 155–164.

Gulley-Stahl, H., Hogan II, P. A., Schmidt, W., Wall, S. J., Buhrlage, A. & Bullen, H. 2010 Surface Complexation of Catechol to Metal Oxides: An ATR-FTIR, Adsorption, and Dissolution Study. *Environ. Sci. Technol.* **44**, 4116–4121.

Gunasekaran, S. & Anbalagan, G. 2007 Spectroscopic study of phase transitions in dolomite mineral. *J. Raman Spectrosc.* **38**, 846–852.

Ho, Y. S. & McKay, G. 1999 Pseudo-second order model for sorption process. *Process Biochem.* **34**, 451–465.

Ji, J., Ge, Y., Balsam, W., Damuth, J. E. & Chen, J. 2009 Rapid identification of dolomite using a Fourier transform infrared spectrophotometer (FTIR): a fast method for identifying Heinrich events in IODP site u1308. *Mar. Geol.* **258**, 60–68.

Johnson, S. B., Hyun Yoon, T., Kocar, B. D., Gordon, E. & Brown, Jr. 2004 Adsorption of organic matter at mineral/water interfaces. 2. Outer-Sphere adsorption of maleate and implications for dissolution processes. *Langmuir* **20**, 4996–5006.

Lagergren, S. 1898 Zur theorie der sogenannten adsorption gelöster stoffe, Kungliga SvenskaVetenskapsademiens. *Handlingar* **24**, 1–39.

Lana-Villarreal, T., Rodes, A., Perez, J. M. & Gomez, R. 2005 A spectroscopic and electrochemical approach to the study of the interactions and photoinduced electron transfer between catechol and anatase nanoparticles in aqueous solution. *J. Am. Chem. Soc.* **127**, 12601–12611.

Langmuir, I. 1918 Adsorption of gases on plane surfaces of glass, mica and platinum. *J. Am. Chem. Soc.* **40**, 1361–1403.

Liao, Q., Sun, J. & Gao, L. 2008 Adsorption of chlorophenols by multiwalled carbon nanotubes treated with $HNO_3$ and $NH_3$. *Carbon* **46**, 553–555.

Madejova, J., Palkova, H. & Komadel, P. 2010 IR spectroscopy of clay minerals and clay nanocomposites. *Spectrosc. Prop. Inorg. Organomet. Compd.* **41**, 22–71.

Mistry, B. D. 2009 *A Handbook of Spectroscopic Data Chemistry*. Oxford Book Company, Jaipur, India.

Moreno-Piraján, J. C., Blanc, D. & Giraldo, L. 2012 Relation between the adsorbed quantity and the immersion enthalpy in catechol aqueous solutions on activated carbons. *Int. J. Mol. Sci.* **13**, 44–55.

Namasivayam, C. & Sumithra, S. 2004 Adsorptive removal of catechol on waste Fe(III)/Cr(III) hydroxide: equilibrium and kinetics study. *Ind. Eng. Chem. Res.* **43**, 7581–7587.

Otsuka, R. 1986 Recent studies on the decomposition of the dolomite group by thermal analysis. *Thermochim Acta* **100**, 183–189.

Pokrovsky, O. S., Mielczarski, J. A., Barres, O. & Schott, J. 2000 Surface speciation models of calcite and dolomite/aqueous solution interfaces and their spectroscopic evaluation. *Langmuir* **16**, 2677–2688.

Redlich, O. & Peterson, D. L. 1959 A useful adsorption isotherm. *J. Phys. Chem.* **63**, 1024–1033.

Rodriguez-Navarro, C., Kudlacz, K. & Ruiz-Agudo, E. 2012 The mechanism of thermal decomposition of dolomite: new insights from 2D-XRD and TEM analyses. *Am. Mineral.* **97**, 38–51.

Saikia, N., Sarma, J., Borah, J. M. & Mahiuddin, S. 2013 Adsorption of 3,4-dihydroxybenzoic acid onto hematite surface in aqueous medium: importance of position of phenolic –OH groups and understanding of the same using catechol as an auxiliary model. *J. Colloid Interface Sci.* **398**, 227–233.

Shahraki, B. K., Mehrabi, B. & Dabiri, R. 2009 Thermal behavior of Zefreh dolomite mine (central Iran). *J. Mining and Metallur.* **45**, 35–44.

Shakir, K., Ghoneimy, H. F., Elkafrawy, A. F., Beheir, S. G. & Refaat, M. 2008 Removal of catechol from aqueous solutions by adsorption onto organophilicbentonite. *J. Hazard. Mater.* **150**, 765–773.

Sharma, V. K., Anquandah, G. A. K., Yngard, R. A., Kim, H., Fekete, J., Bouzek, K., Ray, A. & Golovko, D. 2009 Nonylphenol, octylphenol, and bisphenol-A in the aquatic environment: a review on occurrence, fate, and treatment. *J. Environ. Sci. Health* **A44**, 423–442.

Stefaniak, E., Bilinski, B., Dobrowolski, R., Staszczuk, P. & Wojcik, J. 2002 The influence of preparation conditions on adsorption properties and porosity of dolomite-based sorbents. *Colloids Surf. A* **208**, 337.

Subramanyam, R. & Mishra, I. M. 2007 Biodegradation of catechol (2-hydroxy phenol) bearing wastewater in an UASB reactor. *Chemosphere* **69**, 816–824.

Suresh, S., Srivastava, V. C. & Mishra, I. M. 2011 Study of catechol and resorcinol adsorption mechanism through granular activated carbon characterization, pH and kinetic study. *Sep. Sci. Technol.* **46**, 1750–1766.

Suresh, S., Srivastava, V. C. & Mishra, I. M. 2012 Adsorption of catechol, resorcinol, hydroquinone, and their derivative. A review. *Int. J. of Energy Environ. Eng.* **3**, 32.

Wang, K., Yin, Z., Zhao, P., Han, D., Hu, X. & Zhang, G. 2015 Effect of chemical and physical treatments on the properties of a dolomite used in Ca looping. *Energy Fuels.* **29**, 4428–4435.

Weber, W. J. & Morris, J. C. 1963 Kinetics of adsorption on carbon from solution. *J. Sanitary Eng. Div. Am. Soc. Civ. Eng.* **8**, 31–59.

First received 27 October 2017; accepted in revised form 4 February 2018. Available online 19 February 2018